



## OPEN

Suppression of the two-dimensional electron gas in LaGaO<sub>3</sub>/SrTiO<sub>3</sub> by cation intermixing

S. Nazir, B. Amin &amp; U. Schwingenschlög

KAUST, Physical Science &amp; Engineering Division, Thuwal 23955-6900, Kingdom of Saudi Arabia.

## SUBJECT AREAS:

PHYSICS

CONDENSED-MATTER PHYSICS

NANOSCALE MATERIALS

THEORY AND COMPUTATION

Received

4 October 2013

Accepted

18 November 2013

Published

3 December 2013

Correspondence and requests for materials should be addressed to

U.S. (udo.

schwingenschlog@

kaust.edu.sa)

Cation intermixing at the *n*-type polar LaGaO<sub>3</sub>/SrTiO<sub>3</sub> (001) interface is investigated by first principles calculations. Ti↔Ga, Sr↔La, and SrTi↔LaGa intermixing are studied in comparison to each other, with a focus on the interface stability. We demonstrate in which cases intermixing is energetically favorable as compared to a clean interface. A depopulation of the Ti 3*d*<sub>xy</sub> orbitals under cation intermixing is found, reflecting a complete suppression of the two-dimensional electron gas present at the clean interface.

The high mobility ( $\sim 10^3 \text{ cm}^{-2}\text{V}^{-1}\text{s}^{-1}$  at 4.2 K) two-dimensional electron gas at the (LaO)<sup>+</sup>/(TiO<sub>2</sub>)<sup>0</sup> *n*-type interface<sup>1</sup> between the band insulators LaAlO<sub>3</sub> and SrTiO<sub>3</sub> (STO) is in the focus of interest since quite some time<sup>2–4</sup>. It has been proposed that several mechanisms such as the polar discontinuity<sup>5</sup>, structural relaxation<sup>6</sup>, interdiffusion of cations<sup>7–11</sup>, and oxygen vacancies<sup>12–14</sup>, have to be taken into account to explain the interface conductivity. Of fundamental interest is also the thermodynamic stability of the interface due to the possibility of atomic intermixing in the interface region. Experimentally, cation intermixing of La and Sr at the LaAlO<sub>3</sub>/STO interface has been observed, accompanied by considerable lattice deformations<sup>7</sup>. It is predicted that the interface polarization can be stabilized by the atomic intermixing<sup>15–17</sup>.

Recently, a detail analysis of different configurations of cation intermixing at the *n*-type LaAlO<sub>3</sub>/STO interface has been performed<sup>18</sup>. It has been observed that the energetically most stable configuration is obtained when the interface dipole is cancelled out as a consequence of the cation intermixing. Little further attention has been paid to cation intermixing by first principles theory because of the heavy calculational efforts coming along with the large supercells required for such investigations. However, it has been found that intersite cation La/Sr disorder at the *n*-type LaTiO<sub>3</sub>/STO interface is energetically favorable as compared to an ideal interface, while the electronic properties of the system remain almost the same<sup>19</sup>. On the other hand, the metallic states at the DyScO<sub>3</sub>/STO interface<sup>20</sup> are suppressed for Dy↔Sr and Sc↔Ti intermixing<sup>21</sup>. It has been observed that the dipole energy at the (LaO)<sup>+</sup>/(TiO<sub>2</sub>)<sup>0</sup> interface increases when charge is transferred from the LaO layer to the adjacent STO unit cells<sup>5</sup>. This energy can be reduced by intermixing of the Sr and La cations to produce an electric field which compensates the interface dipole.

In this work, we study Ti↔Ga, Sr↔La, and SrTi↔LaGa cation intermixing at the *n*-type (LaO)<sup>+</sup>/(TiO<sub>2</sub>)<sup>0</sup> interface between LaGaO<sub>3</sub> (LGO) and STO. Formation of a two-dimensional electron gas at this interface has been reported experimentally and the effect of O vacancies on the conductivity has been addressed in Refs. 22–24. Metallic states appear for both the *n* and *p*-type LGO/STO interfaces, where the metallicity of the *n*-type interface is enhanced by O vacancies. On the other hand, the *p*-type interface turns gradually from a hole doped into an electron doped state for strong O deficiency<sup>25</sup>. Polar distortion effects have been studied theoretically in Ref. 26.

## Results

The bulk electronic structures of LGO and STO are well understood. Since the lattice mismatch between the component materials is small, the structural relaxation at the interface does not play a dominating role. LGO has a pseudocubic structure with an experimental lattice constant of 3.874 Å, whereas STO has cubic structure with an experimental lattice constant of 3.905 Å. We model the TiO<sub>2</sub>/LaO interface by means of a supercell approach, using the average value of these two lattice constants, i.e., 3.884 Å. We start from the 6 unit cells of STO, containing 120 atoms, and stack 4 unit cells of LGO, contain 80 atoms, on top along the (001) direction. After the two slabs we place along the (001) direction a vacuum slab of 15 Å thickness. This gives rise to an asymmetric model. The supercell contains a total of 200 atoms, of which 16, 24, 16, 24, and 120 are La, Sr, Ga, Ti, and O,



respectively. A TiO<sub>2</sub> layer with four Ti atoms forms the interface to the first LaO layer of the LGO slab. Besides the asymmetric model, we also address a symmetric model with a total of 292 atoms (32 La, 24 Sr, 32 Ga, 28 Ti, and 176 O), for which we again apply a vacuum slab of 15 Å thickness. If not stated otherwise, the following results are obtained in both the symmetric and asymmetric models. It has been found experimentally that the roughness of the interface (i.e., the depth of the cation intermixing) is approximately 2 unit cells for the *n*-type LaAlO<sub>3</sub>/STO and LaVO<sub>3</sub>/STO interfaces<sup>5,7,27,28</sup>, whereas according to Ref. 18 for the LaAlO<sub>3</sub>/STO interface a deeper intermixing might affect the LaAlO<sub>3</sub> region.

The energy required for or gained by cation intermixing is calculated as  $\Delta E = E_{\text{ideal}} - E_{\text{intermixed}}$ , where  $E_{\text{ideal}}$  is the energy of the ideal interface and  $E_{\text{intermixed}}$  is the total energy obtained for a supercell in which cations have been exchanged. A positive value of  $\Delta E$  corresponds to a stable state after intermixing. Schematic representations of the ideal interface structure and different configurations with cation intermixing are shown in Fig. 1. In each case, 25% of the atoms in the layers affected by intermixing are exchanged. In Fig. 1 we show only configurations in which the intermixing is restricted to the atomic layers directly at the interface, while we will study in the following also diffusion into layers further off the interface. Since the lattice relaxation is essential at disordered interfaces, a full relaxation of all supercells is required.

It turns out that the stability (energy gain or loss) of a specific intermixing depends on the positions of the exchanged impurity atoms. For the Ti $\leftrightarrow$ Ga intermixing, we first exchange one interface Ti atom with a Ga atom in the 1st, 2nd, 3rd, or 4th LGO unit cell (counted from the interface) and then exchange one interface Ga atom with a Ti atom in the 1st, 2nd, 3rd, or 4th STO unit cell. The same exchange scheme is applied for the Sr $\leftrightarrow$ La and SrTi $\leftrightarrow$ LaGa intermixing. The calculated values of  $\Delta E$  for Ti $\leftrightarrow$ Ga intermixing are summarized in Fig. 2. Figure 2(a) shows that when an interface Ti atom is exchanged with Ga in the 1st LGO unit cell the system is stabilized by 0.06 eV. Similarly, the energy gains for exchange with Ga in the 2nd, 3rd, and 4th LGO unit cell are 0.21 eV, 0.29 eV, and 1.24 eV, respectively. The longer the distance to the interface the higher is therefore the energy gain. A similar pattern of the energy gain has been obtained for the LaAlO<sub>3</sub>/STO interface<sup>4</sup>, because the intermixing induces an electric field which compensates the interface dipole and thus reduces the energy of the system<sup>17</sup>. This effect is demonstrated in Fig. 3, in which we compare the electrostatic potentials obtained for the ideal and intermixed interfaces. According to Fig. 2(b), exchange of an interface Ga atom with Ti in the 2nd, 3rd, and 4th STO unit cell destabilizes the system. The energy losses

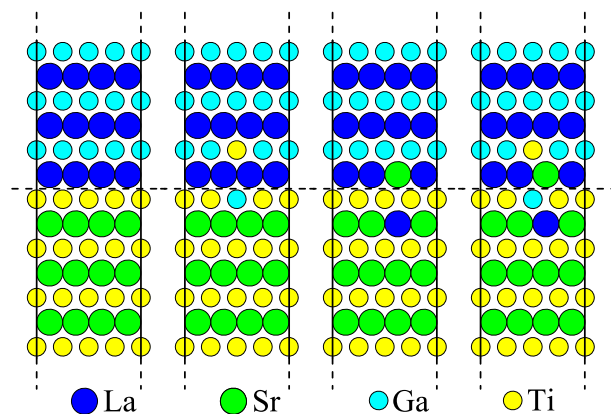


**Figure 1** | Structural configurations considered at the LGO/STO interface, from left to right: ideal, Ti $\leftrightarrow$ Ga intermixing, Sr $\leftrightarrow$ La intermixing, and SrTi $\leftrightarrow$ LaGa intermixing, in each case directly at the interface.

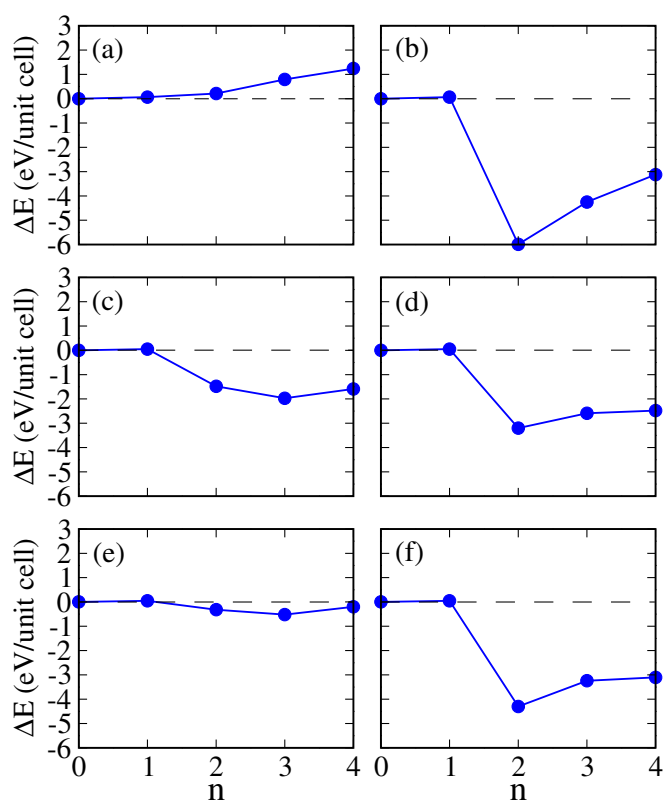


**Figure 2** | Total energy difference induced by the cation intermixing: (a) Exchange of an interface Ti atom with a Ga atom in the *n*-th LGO unit cell, (b) exchange of an interface Ga atom with a Ti atom in the *n*-th STO unit cell, (c) exchange of an interface Sr atom with a La atom in the *n*-th LGO unit cell, (d) exchange of an interface La atom with a Sr atom in the *n*-th STO unit cell, (e) exchange of an interface SrTi pair with a LaGa pair in the *n*-th LGO unit cell, and (f) exchange of an interface LaGa pair with a SrTi pair in the *n*-th STO unit cell. By  $n = 0$  we denote the ideal unit cell.

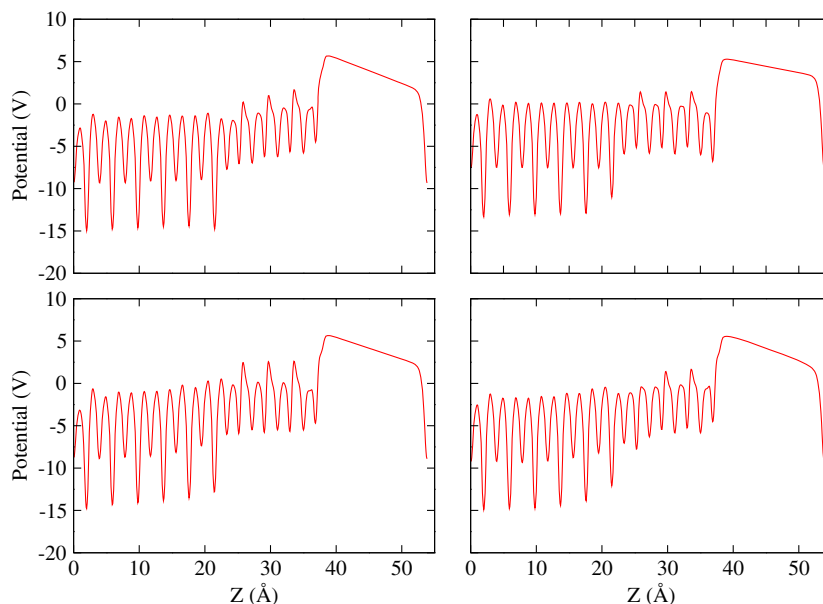
amount to  $-5.99$  eV,  $-4.25$  eV, and  $-3.12$  eV. While Ti diffusion into the LGO thus is energetically favorable, Ga diffusion into the STO is not. The authors of Ref. 22 report a Ti signal past the interface on the LGO side and note that this could be due to Ti diffusion. While this scenario would agree with our findings, those authors believe that the signal is rather due to pollution introduced during the sample preparation.

Figure 2(c) deals with Sr $\leftrightarrow$ La intermixing. Exchange of an interface Sr atom with La in the 1st LGO unit cell leads to an energy gain of 0.05 eV. A similar stability is found for La/Sr disorder at the *n*-type LaTiO<sub>3</sub>/STO and LaAlO<sub>3</sub>/STO interfaces<sup>19,29</sup>. For deeper diffusion of Sr into the LGO, the total energy is higher than that of the ideal system. For  $\Delta E$  we obtain  $-1.45$  eV,  $-2.32$  eV, and  $-2.83$  eV for incorporation in the 2nd, 3rd, and 4th LGO unit cell, respectively. Moreover, exchange of an interface La atom with a Sr atom in the 2nd, 3rd, and 4th STO unit cell leads to energy losses of  $-3.20$  eV,  $-2.59$  eV, and  $-2.48$  eV, respectively. We obtain the most stable state when La and Sr are exchanged directly at the interface. While La diffuses further into the STO, Sr diffusion into the LGO is not possible. The coupled SrTi $\leftrightarrow$ LaGa cation intermixing, i.e., exchange of SrTi and LaGa pairs, is addressed in Figs. 2(e) and 2(f). We obtain an energy gain only when the exchange occurs directly at the interface. While cooperative diffusion of SrTi into the LGO is possible, diffusion of LaGa into the STO is energetically not favorable.

Orbitally resolved Ti *3d* densities of states (DOSs) for different interface configurations are shown in Fig. 4 to address the influence of the cation intermixing on the electronic structure. The top row gives results for the ideal interface and for Ti $\leftrightarrow$ Ga intermixing in the



### Asymmetric model



### Symmetric model

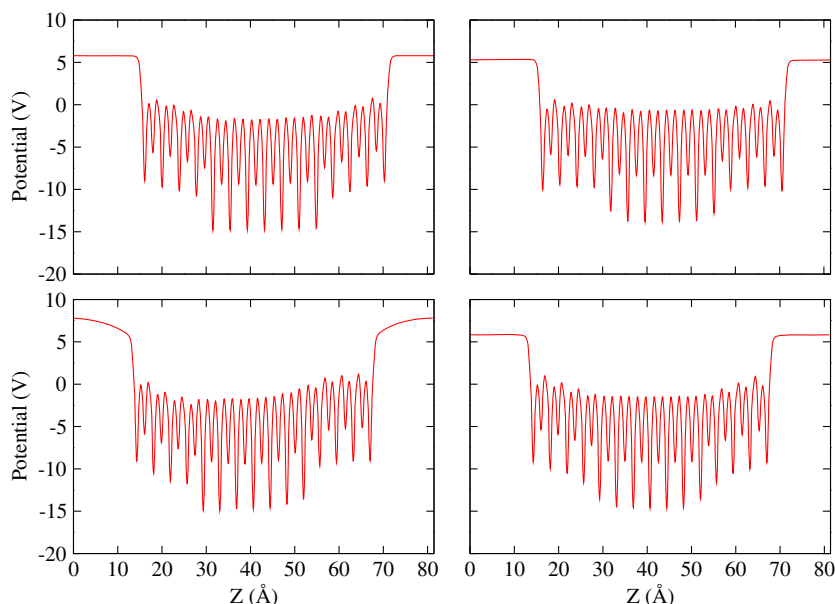


**Figure 3** | Electrostatic potential, referring to the most stable configurations of the (top left) ideal interface, (top right) Ti↔Ga exchange, (bottom left) Sr↔La exchange, and (bottom right) SrTi↔LaGa exchange.

4th LGO unit cell (most stable configuration), respectively. Clearly, Ti↔Ga intermixing has a significant effect on the interface conductivity. The Ti states shift to higher energy and become completely depopulated, which gives rise to a large band gap. DOSs obtained for Sr↔La and SrTi↔LaGa intermixing (most stable configurations) are shown in the bottom row of Fig. 4. They reveal almost the same features as obtained for Ti↔Ga intermixing, but with smaller band gaps.

In general, the crystal field due to the octahedral coordination by O atoms splits the Ti 3d states into high energy  $e_g$  ( $d_{3z^2-r^2}$  and  $d_{x^2-y^2}$ ) and low energy  $t_{2g}$  ( $d_{xy}$ ,  $d_{xz}$ , and  $d_{yz}$ ) states. Note that the O octahedron is distorted at the interface and the crystal field therefore is not perfectly octahedral. In case of the clean interface the  $d_{xy}$  orbital (which is oriented parallel to the interface) is occupied and therefore carries the two-dimensional electron gas. The remaining  $t_{2g}$  orbitals

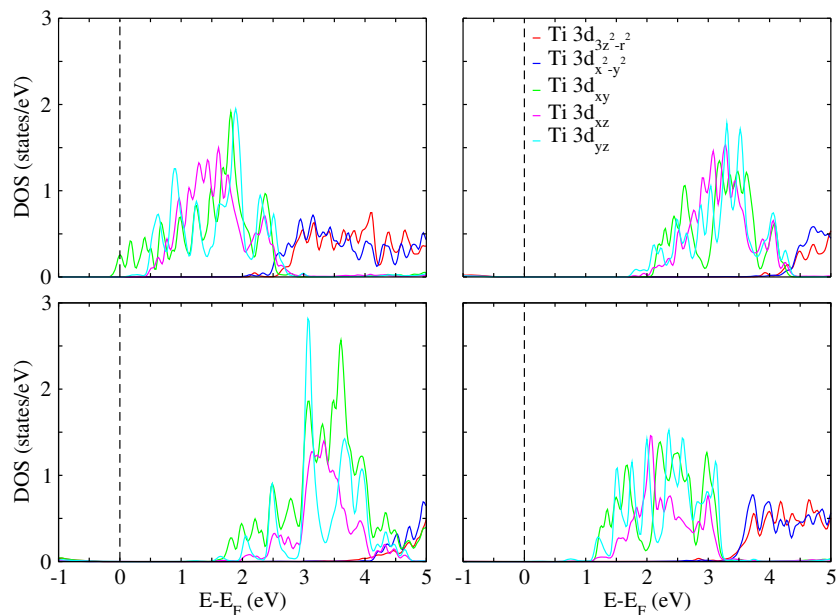
( $d_{xz}$  and  $d_{yz}$ ) are degenerate and occupy the energy range from slightly above  $E_F$  up to about 3 eV. The  $e_g$  orbitals stay far above  $E_F$  and therefore play no role for the interface metallicity. The charge carrier density in the  $d_{xy}$  orbitals amounts to  $3.4 \cdot 10^{13} \text{ cm}^{-2}$ ,  $1.6 \cdot 10^{13} \text{ cm}^{-2}$ , and  $0.1 \cdot 10^{13} \text{ cm}^{-2}$  in the 1st, 2nd, and 3rd  $\text{TiO}_2$  layer from the interface. Rather similar shapes of the orbitally resolved DOSs are obtained for Ti↔Ga intermixing, for Sr↔La intermixing, and for SrTi↔LaGa intermixing, see Fig. 4. However, in each of these cases the states appear at much higher energy and no metallicity is induced.

### Discussion

Let us now turn to the question why cation intermixing in  $\text{LaGaO}_3/\text{STO}$  results in a suppression of the interface metallicity, while in



## Asymmetric model



## Symmetric model

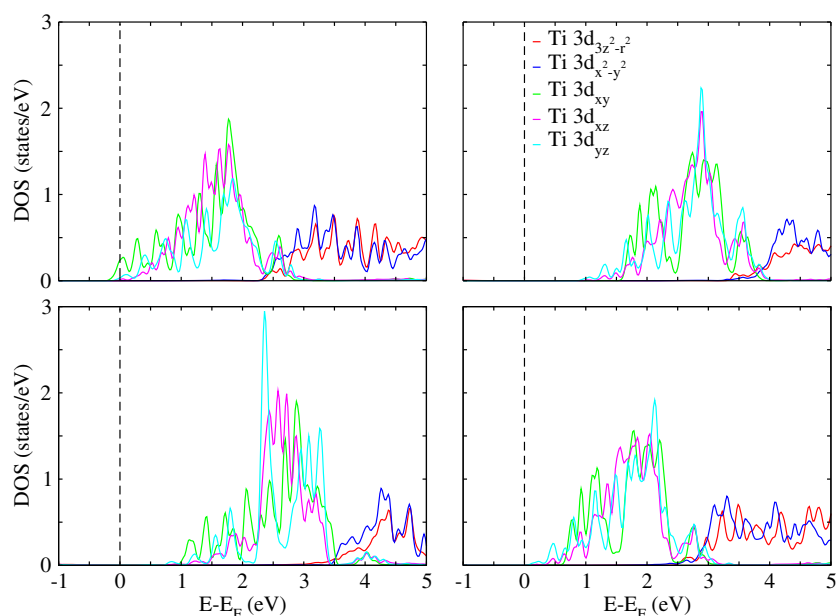


**Figure 4** | Orbitaly resolved partial  $3d$  DOS of the interface Ti atom next to the site where an atom has been exchanged, referring to the most stable configurations of the (top left) ideal interface, (top right)  $\text{Ti} \Leftrightarrow \text{Ga}$  exchange, (bottom left)  $\text{Sr} \Leftrightarrow \text{La}$  exchange, and (bottom right)  $\text{SrTi} \Leftrightarrow \text{LaGa}$  exchange.

$\text{LaTiO}_3/\text{STO}$  no such effect is found<sup>19</sup>. We focus on the first  $\text{TiO}_2$  layer directly at the interface. As  $\text{Ti-O-Ti}$  bonding is replaced by  $\text{Ti-O-Ga}$  bonding, differences in the electronegativity between Ti and Ga are expected to have important implications. A Ga atom contributes less charge to the covalent  $\text{Ga-O}$  bond due to its high electronegativity of 1.81, as compared to the Ti electronegativity of 1.54. As a consequence, the orbital overlap between Ti and O is reduced and delocalized states within the modified  $\text{TiO}_2$  layer become energetically less favorable (the band width of the  $d_{xy}$  states decreases). In addition, the ionic nature of the bonds will also influence neighbouring atoms so that a rather small amount of impurities can strongly counteract the creation of the two-dimensional electron gas. In the case of  $\text{Sr} \Leftrightarrow \text{La}$  intermixing we have to take into account that the electronegativity of Sr (0.95) is smaller than that of La (1.1),

although the difference of 0.15 between Sr and La is smaller than the difference of 0.27 between Ti and Ga. This effect can clearly be seen in the DOS. The band gap for  $\text{Ti} \Leftrightarrow \text{Ga}$  intermixing is larger than for  $\text{Sr} \Leftrightarrow \text{La}$  intermixing, which confirms that the cation electronegativity plays an important role for the two-dimensional electron gas at perovskite oxide interfaces. Therefore, the suppression of the two-dimensional electron gas by cation intermixing is a consequence of an enhanced ionic character of the metal-O bonds and the induced electric field that compensates the interface dipole.

In conclusion, we have studied the stability and electronic structure of the  $n$ -type LGO/STO interface by first principles calculations. We find a two-dimensional electron gas for the ideal interface, while the interfaces for  $\text{Ti} \Leftrightarrow \text{Ga}$ ,  $\text{Sr} \Leftrightarrow \text{La}$ , and  $\text{SrTi} \Leftrightarrow \text{LaGa}$  intermixing exhibit insulating states. All three types of intermixing can result in



an energy gain and therefore in thermodynamic stability. The energy gain or loss due to the cation intermixing depends strongly on the distance of the exchanged ions from the interface. Importantly, the interface electronic structures of the cation intermixed configurations are all characterized by a complete suppression of the two-dimensional electron gas present at the clean interface. This fact demonstrates the key role of an atomically clean interface to obtain a two-dimensional electron gas.

## Methods

Our calculations are performed in the framework of spin-degenerate density functional theory using the generalized gradient approximation in the Perdew-Wang flavor and projector augmented wave pseudopotentials, as implemented in the Vienna Ab-initio Simulation Package. The presented results have been obtained without onsite Coulomb interaction. However, we have checked the metallic cases for an onsite interaction of  $U = 4$  eV on the Ti  $3d$  orbitals and find no qualitative difference. Relativistic effects are taken into account fully for the core states, while the scalar relativistic approximation is used for the valence states (i.e., spin-orbit coupling is neglected). The electronic wave function is expanded with a kinetic energy cutoff of 400 eV. We optimize the crystal structures by minimizing the atomic forces until all residual forces remain below  $0.001$  eV/Å. A  $10 \times 10 \times 1$   $k$ -space grid, comprising 21 points in the irreducible wedge of the Brillouin zone, is found to be well converged. Self-consistency is assumed for a total energy convergence below  $0.0001$  eV. Moreover, the DOS is calculated with a Gaussian smearing of  $0.05$  eV.

- Ohtomo, A. & Hwang, H. Y. A high-mobility electron gas at the LaAlO<sub>3</sub>/SrTiO<sub>3</sub> heterointerface. *Nature* **427**, 423–426 (2004).
- Pauli, S. A. & Willmott, P. R. Conducting interfaces between polar and non-polar insulating perovskites. *J. Phys.: Condens. Matter* **20**, 264012 (2008).
- Pentcheva, R. & Pickett, W. E. Electronic phenomena at complex oxide interfaces: insights from first principles. *J. Phys.: Condens. Matter* **22**, 043001 (2010).
- Chambers, S. A. *et al.* Instability, intermixing and electronic structure at the LaAlO<sub>3</sub>/SrTiO<sub>3</sub> (001) epitaxial heterojunction. *Surf. Sci. Rep.* **65**, 317–352 (2010).
- Nakagawa, N., Hwang, H. Y. & Muller, D. A. Why some interfaces cannot be sharp. *Nature Mater.* **5**, 204–209 (2006).
- Schwingschlögl, U. & Schuster, C. Exponential decay of relaxation effects at LaAlO<sub>3</sub>/SrTiO<sub>3</sub> heterointerfaces. *Chem. Phys. Lett.* **467**, 354–357 (2009).
- Willmott, P. R. *et al.* Structural basis for the conducting interface between LaAlO<sub>3</sub> and SrTiO<sub>3</sub>. *Phys. Rev. Lett.* **99**, 155502 (2007).
- Kalabukhov, A. S. *et al.* Cationic disorder and phase segregation in LaAlO<sub>3</sub>/SrTiO<sub>3</sub> heterointerfaces evidenced by medium-energy ion spectroscopy. *Phys. Rev. Lett.* **103**, 146101 (2009).
- Huijben, M. *et al.* Structure-property relation of SrTiO<sub>3</sub>/LaAlO<sub>3</sub> interfaces. *Adv. Mater.* **21**, 1665–1677 (2009).
- Kalabukhov, A. S. *et al.* Improved cationic stoichiometry and insulating behavior at the interface of LaAlO<sub>3</sub>/SrTiO<sub>3</sub> formed at high oxygen pressure during pulsed-laser deposition. *EPL* **93**, 37001 (2011).
- Vonk, V. *et al.* Polar-discontinuity-retaining A-site intermixing and vacancies at SrTiO<sub>3</sub>/LaAlO<sub>3</sub> interfaces. *Phys. Rev. B* **85**, 045401 (2012).
- Thiel, S., Hammerl, G., Schmehl, A., Schneider, C. W. & Mannhart, J. Tunable quasi-two-dimensional electron gases in oxide heterostructures. *Science* **313**, 1942–1945 (2006).
- Takizawa, M. *et al.* Photoemission from buried interfaces in SrTiO<sub>3</sub>/LaTiO<sub>3</sub> superlattices. *Phys. Rev. Lett.* **97**, 057601 (2006).
- Park, M. S., Rhim, S. H. & Freeman, A. J. Charge compensation and mixed valency in LaAlO<sub>3</sub>/SrTiO<sub>3</sub> heterointerfaces studied by the FLAPW method. *Phys. Rev. B* **74**, 205416 (2006).
- Popović, Z. S., Satpathy, S. & Martin, R. M. Origin of the two-dimensional electron gas carrier density at the LaAlO<sub>3</sub> on SrTiO<sub>3</sub> interface. *Phys. Rev. Lett.* **101**, 256801 (2008).
- Pentcheva, R. & Pickett, W. E. Avoiding the polarization catastrophe in LaAlO<sub>3</sub> overlayers on SrTiO<sub>3</sub>(001) through polar distortion. *Phys. Rev. Lett.* **102**, 107602 (2009).
- Yamamoto, R. *et al.* Structural comparison of n-type and p-type LaAlO<sub>3</sub>/SrTiO<sub>3</sub> interfaces. *Phys. Rev. Lett.* **107**, 036104 (2011).
- Qiao, L. *et al.* Thermodynamic instability at the stoichiometric LaAlO<sub>3</sub>/SrTiO<sub>3</sub>(001) interface. *J. Phys.: Condens. Matter* **22**, 312201 (2010).
- Pulikkotil, J. J., Auluck, S., Kumar, P., Dogra, A. & Budhani, R. C. Energetics and electronic structure of La/Sr disorder at the interface of SrTiO<sub>3</sub>/LaTiO<sub>3</sub> heterostructure. *Appl. Phys. Lett.* **99**, 081915 (2011).
- Li, D. F., Wang, Y. & Dai, J. Y. Tunable electronic transport properties of DyScO<sub>3</sub>/SrTiO<sub>3</sub> polar heterointerface. *Appl. Phys. Lett.* **98**, 122108 (2011).
- Rahmanizadeh, K., Bihlmayer, G., Luysberg, M. & Blügel, S. First-principles study of intermixing and polarization at the DyScO<sub>3</sub>/SrTiO<sub>3</sub> interface. *Phys. Rev. B* **85**, 075314 (2012).
- Perna, P. *et al.* Conducting interfaces between band insulating oxides: The LaGaO<sub>3</sub>/SrTiO<sub>3</sub> heterostructure. *Appl. Phys. Lett.* **97**, 152111 (2010).
- Aruta, C. *et al.* Pulsed laser deposition of SrTiO<sub>3</sub>/LaGaO<sub>3</sub> and SrTiO<sub>3</sub>/LaAlO<sub>3</sub>: Plasma plume effects. *Appl. Phys. Lett.* **97**, 252105 (2010).
- Aruta, C. *et al.* Critical influence of target-to-substrate distance on conductive properties of LaGaO<sub>3</sub>/SrTiO<sub>3</sub> interfaces deposited at  $10^{-1}$  mbar oxygen pressure. *Appl. Phys. Lett.* **101**, 031602 (2012).
- Nazir, S., Singh, N. & Schwingschlögl, U. The metallic interface between the two band insulators LaGaO<sub>3</sub> and SrTiO<sub>3</sub>. *Appl. Phys. Lett.* **98**, 262104 (2011).
- Xu, Q., Wu, D. & Li, A. Effect of polar distortion on the electronic structure of (001) LaGaO<sub>3</sub>/SrTiO<sub>3</sub> interface. *Phys. Lett. A* **377**, 577–581 (2013).
- Kourkoutis, L. F., Muller, D. A., Hotta, Y. & Hwang, H. Y. Asymmetric interface profiles in LaVO<sub>3</sub>/SrTiO<sub>3</sub> heterostructures grown by pulsed laser deposition. *Appl. Phys. Lett.* **91**, 163101 (2007).
- Jia, C. L. *et al.* Oxygen octahedron reconstruction in the SrTiO<sub>3</sub>/LaAlO<sub>3</sub> heterointerfaces investigated using aberration-corrected ultrahigh-resolution transmission electron microscopy. *Phys. Rev. B* **79**, 081405(R) (2009).
- Zhong, Z., Xu, P. X. & Kelly, P. J. Polarity-induced oxygen vacancies at LaAlO<sub>3</sub>/SrTiO<sub>3</sub> interfaces. *Phys. Rev. B* **82**, 165127 (2010).

## Acknowledgments

We thank L.-Y. Gan for fruitful discussions and KAUST research computing for providing the computational resources used for this investigation.

## Author contributions

S.N. and B.A. conducted the calculations. S.N. and U.S. wrote the manuscript.

## Additional information

**Competing financial interests:** The authors declare no competing financial interests.

**How to cite this article:** Nazir, S., Amin, B. & Schwingschlögl, U. Suppression of the two-dimensional electron gas in LaGaO<sub>3</sub>/SrTiO<sub>3</sub> by cation intermixing. *Sci. Rep.* **3**, 3409; DOI:10.1038/srep03409 (2013).



This work is licensed under a Creative Commons Attribution-NonCommercial-NoDerivs 3.0 Unported license. To view a copy of this license, visit <http://creativecommons.org/licenses/by-nc-nd/3.0>